Published in final edited form as:
Biol Cybern. 2004 October ; 91(4): 231–242. doi:10.1007/s00422-004-0506-2.

Prehension synergies during nonvertical grasping, II: Modeling and optimization

Todd C. Pataky, **Mark L. Latash**, and **Vladimir M. Zatsiorsky**
Biomechanics Laboratory, 39 Recreation Building, The Pennsylvania State University, University Park, PA 16802, USA

Abstract

This study examines various optimization criteria as potential sources of constraints that eliminate (or at least reduce the degree of) mechanical redundancy in prehension. A model of nonvertical grasping mimicking the experimental conditions of Pataky et al. (current issue) was developed and numerically optimized. Several cost functions compared well with experimental data including energylike functions, entropylike functions, and a “motor command” function. A tissue deformation function failed to predict finger forces. In the prehension literature, the “safety margin” (SM) measure has been used to describe grasp quality. We demonstrate here that the SM is an inappropriate measure for nonvertical grasps. We introduce a new measure, the “generalized safety margin” (GSM), which reduces to the SM for vertical and two-digit grasps. It was found that a close-to-constant GSM accounts for many of the finger force patterns that are observed when grasping an object oriented arbitrarily with respect to the gravity field. It was hypothesized that, when determining finger forces, the CNS assumes that a grasped object is more slippery than it actually is. An “operative friction coefficient” of approximately 30% of the actual coefficient accounted for the offset between experimental and optimized data. The data suggest that the CNS utilizes an optimization strategy when coordinating finger forces during grasping.

1 Introduction

This paper is a sequel to Pataky et al. (2004a). Part I investigated digit forces while holding an object at various orientations with respect to the gravity field. The purposes of Part II are: (1) to elaborate on the mechanical peculiarities of nonvertical grasping and (2) to offer an explanation for the experimental results of Part I. The explanation is based on mechanical optimization of a model that describes the investigated task. In the interest of compactness, experimental results for only the four-finger task from Part I will be used to complement the current optimization discussion.

Despite its static indeterminacy, subjects perform multifinger grasping in a highly reproducible way (e.g., Li et al. 1998) when presented with a particular set of mechanical demands. While intertrial variability exists, this variability is smaller than the variability associated with changing the mechanical demands (e.g., Li et al. 1998). The fact that performance is repeatable across load magnitudes (Shim et al. 2003) indicates that similar mechanical demands beget similar CNS responses.

It is conceivable that the CNS produces digit forces according to some objective optimization criterion or criteria. The physiological basis for this contention is the fact that neuron activity

Correspondence to: T. Pataky, (tcp120@psu.edu, Tel.: +1-814-8653445, Fax: +1-814-8652441).

level is related to mechanical variables that are manifested externally. That is, increasing alpha-motoneuron activity naturally increases muscle forces, while reducing this activity conserves energetic resources. Additionally, the strong coupling of afferents and alpha-motoneurons serving the hand (McNulty et al. 1999) implies that external mechanical variables may directly influence finger forces via spinal circuits without substantial supraspinal involvement and conscious perception. Regardless of the possible physiological mechanisms, optimization is attractive for addressing prehension's static indeterminacy because it could constitute the constraint equations that would render the system solvable – thus leading to reproducible performance. Previous research on prehension has found qualitative agreement between experimental observations and optimization's predictions (Hershkovitz et al. 1997; Zatsiorsky et al. 2002).

For a pinch grasp with vertical object orientation, the simplest optimization scheme would be to assign normal forces (F_n) the minimum value to prevent slip. However, it has been widely documented that the CNS does not employ this technique (e.g., Westling and Johansson 1984; Burstedt et al. 1999; Li 2002). Moreover, for more than two digits, this scheme does not provide a unique solution. The "safety margin" (SM) has been used in the literature to address this issue. Conceptually, the SM relates the observed F_n to the task-dependent minimum F_n. The SM was introduced for two-finger grasps (Westling and Johansson 1984) and was defined as the difference between the observed F_n and the F_n required forces to prevent slip. If the CNS specifies a constant SM, the pinch problem is solved (but only for vertical object orientation, i.e., when only tangential forces contribute to weight support). For more than two digits this scheme does not provide a unique solution. While the SM has been examined for more than two fingers (Burstedt et al. 1999), its relation to the corresponding static indeterminacy has not been addressed. Importantly, for nonvertical object orientations the SM, as it is defined in the literature, is ambiguous (Sect. 4.2). However, as will be discussed later, the SM concept can be extended to the general grasping task if, rather than specifying the F_n required to prevent slip, the "required" forces are defined on the basis of a mechanically optimum solution.

The current study thus examines various optimization criteria as potential sources for constraint equations that eliminate (or at least reduce the degree of) indeterminacy in prehension. New grasping control variables are proposed: generalized safety margin (GSM) and operative friction coefficient (μ_{op}). It was found that these optimization-based variables account for many of the finger force patterns that are observed during nonvertical grasping.

The paper is structured as follows. In Sect. 2 a mechanical model of nonvertical grasping is developed. The procedures and results of optimization in which five different cost functions were employed are described in Sect. 3. The mechanical peculiarities of nonvertical grasping are discussed in Sect. 4, and a summary discussion is provided in Sect. 5.

2 Model of nonvertical grasping

Consider the planar equilibrium of a grasped object with weight W. Two coordinate systems are defined as follows: normal (n) and tangential (t) object axes are coincident with the global horizontal (X) and vertical (Y) axes, respectively, for $\theta = 0$, where θ is the angle between t and Y as defined by a right-handed coordinate system (see Fig. 1 for a description of all notation). The digit forces are denoted as: $(F_q)_i$ where q represents the axis of interest and the subscript i refers to any of the five digits – thumb (T), index (I), middle (M), ring (R), or little (L) – or to the "virtual finger" (VF). The VF is an imagined finger that produces a wrench equal to the wrenches produced by all of the fingers (Arbib et al. 1985;Iberall 1986). The point of application of F_{VF} depends on the distribution of finger forces.

To establish an algebraic basis for optimization, the constraints of object equilibrium must be considered. For planar static grasping there are three equilibrium equations to satisfy:

$$\sum_{i=1}^{N}(F_n)_i = W_n, \tag{1}$$

$$\sum_{i=1}^{N}(F_t)_i = W_t, \tag{2}$$

$$\sum_{i=1}^{N}(M_{nt})_i = M_{\text{ext}}, \tag{3}$$

where N is the number of digits used ($2 \leq N \leq 5$), M_{nt} represents the moments exerted in the n–t plane, M_{ext} is the negative of the external moment acting on the handle (or the resultant moment necessary to maintain equilibrium), and W_n and W_t are the projections of the object's weight on the n and t axes, respectively:

$$W_n = \sin|\theta|, \tag{4}$$

$$W_t = \cos\theta. \tag{5}$$

Assuming hard finger–object contacts (i.e., point contact with friction and no contact couples) and Coulomb friction, the normal forces $(F_n)_i$ are also subject to the following no-slip constraint:

$$(F_n)_i \geq (\mu_i)^{-1}|(F_t)_i|, \tag{6}$$

where μ_i is the coefficient of static friction between the ith finger and the grasped object. Equations (1-3) and (6) may be expressed as a set of linear constraints in matrix form as follows:

$$\mathbf{AF} \leq \mathbf{S}, \tag{7}$$

$$\mathbf{A_{eq}F} = \mathbf{L}, \tag{8}$$

where (7) represents the no-slip constraints (6) and (8) represents the equilibrium constraints (2) and (3). Equations (7) and (8) collectively constitute a force closure (i.e., all solutions that simultaneously satisfy both equations represent static equilibrium). The vector $\boldsymbol{F}$ is the (2 N×1) vector of digit forces:

$$\mathbf{F} = \begin{bmatrix} \mathbf{F_n} \\ \mathbf{F_t} \end{bmatrix}$$

which implies that:

$$F(i) = (F_n)_i$$
$$F(i+N) = (F_t)_i$$

where i is the ith finger and $F(i)$ is the ith element of $\boldsymbol{F}$. Note that $\boldsymbol{F}$ is *not* the resultant force produced by the vector sum of $\boldsymbol{F}_n$ and $\boldsymbol{F}_t$. The vector $\boldsymbol{S}$ is the ($2N \times 1$) zero vector that constitutes the no-slip inequality constraints and $\boldsymbol{L}$ is the (3×1) load vector that constitutes the right-hand side of the equilibrium constraints (1)-(3):

$$\mathbf{L} = [W_n, W_t, M_{\text{ext}}]^{\mathrm{T}}.$$

The matrix $\boldsymbol{A}$ is a ($2N \times 2N$) square matrix, and the matrix $\boldsymbol{A}_{\mathbf{eq}}$ is ($3 \times 2N$). Both are best defined by example: if the T, I, and M digits are used to grasp the object shown in Fig. 1, the terms of (7) and (8) expand to:

$$\mathbf{F} = \left[(F_n)_{\mathrm{T}}, (F_n)_{\mathrm{I}}, (F_n)_{\mathrm{M}}, (F_t)_{\mathrm{T}}, (F_t)_{\mathrm{I}}, (F_t)_{\mathrm{M}}\right]^{\mathrm{T}},$$
$$\mathbf{S} = [0, 0, 0, 0, 0, 0]^{\mathrm{T}},$$
$$\mathbf{L} = [W_n, W_t, M_{\text{ext}}]^{\mathrm{T}},$$
$$\boldsymbol{A} = \begin{bmatrix} -\mu_{\mathrm{T}} & 0 & 0 & 1 & 0 & 0 \\ 0 & -\mu_{\mathrm{I}} & 0 & 0 & 1 & 0 \\ 0 & 0 & -\mu_{\mathrm{M}} & 0 & 0 & 1 \\ -1 & 0 & 0 & 0 & 0 & 0 \\ 0 & -1 & 0 & 0 & 0 & 0 \\ 0 & 0 & -1 & 0 & 0 & 0 \end{bmatrix},$$
$$\boldsymbol{A}_{\mathbf{eq}} = \begin{bmatrix} 1 & -1 & -1 & 0 & 0 & 0 \\ 0 & 0 & 0 & 1 & 1 & 1 \\ (r_n)_{\mathrm{T}} & (r_n)_{\mathrm{I}} & (r_n)_{\mathrm{M}} & (r_t)_{\mathrm{T}} & (r_t)_{\mathrm{I}} & (r_t)_{\mathrm{M}} \end{bmatrix},$$

where $(r_n)_i$ and $(r_t)_i$ are the moment arms of the normal and tangential forces, respectively. For compactness, moments are computed about the origin of the n–t coordinate system illustrated in Fig. 1 (i.e., such that W does not produce a moment). The moment arms $(r_n)_i$ and $(r_t)_i$ can be expressed as ($1 \times N$) vectors $\boldsymbol{r_n}$ and $\boldsymbol{r_t}$. The coefficients μ_i were considered to be 1.4 for all digits [F. Gao (2002), unpublished M.S. thesis, The Pennsylvania State University]. Equations (7) and (8) constitute the full set of mechanical constraints to be submitted to an optimization routine.

3 Optimization procedure and results

3.1 Procedure

The optimization problem was formulated in terms of design variables $\boldsymbol{F}$ as follows:

$$\text{minimize} \quad \{f(\boldsymbol{F})) : \boldsymbol{F} \in \Omega\}$$

where $\Omega = \{\boldsymbol{F} : g_j(\boldsymbol{F}) \leq 0, h_k(\boldsymbol{F}) = 0\}$; $j = 1, \ldots, 2N$; $k = 1, 2, 3$.

The function f is a cost function, and the g_j's and h_k's are the inequality and equality constraints, respectively, that are described by (7) and (8). The set Ω is the feasible solution region defined by the constraints. Geometrically Ω represents the intersection of the h_k's (which are $2N$-dimensional hyperplanes) that is truncated by the g_j's. Importantly, the Ω described by (5) and

(6) is a convex set. This is due to the fact that all g_j's are convex and all h_k's are linear (Burstedt et al. 1999). Thus, where f is a convex function, the optimization problem itself is convex and a local minimum is, in fact, the global minimum.

Five cost functions $f(\boldsymbol{F})$ were selected on the basis of intuition or their previous use in the prehension literature (e.g., Hershkovitz et al. 1995, 1997). All were convex except one (Sect. 3.1.5). Each is addressed separately below in Sects. 3.1.1–3.1.5. All objective functions were tested for either all N digits or all fingers (i.e., N–1 digits excluding T). In all cases $M_{\text{ext}} = 0$ and $\mu_i = \mu = 1.4$ for all digits.

All optimization problems were solved using the procedure *fmincon* from MATLAB's optimization toolbox (The MathWorks Inc., Natick, MA, USA). The optimum ($\boldsymbol{F}_*$) results were unaffected by random variations in initial ($\boldsymbol{F}^0$) values submitted to the routines.

3.1.1 Energylike function over F—A measure that is proportional to the potential energy of deformation for a linear (i.e., Hookian) system has been used widely in the literature, for example, as a component of the human grasping quality sense (Hershkovitz et al. 1997):

$$f_1 = \sum_{i=i_0}^{N} (F_r)_i^2,$$

where $(F_r)_i$ is the magnitude of the vector sum $|(\boldsymbol{F}_n)_i + (\boldsymbol{F}_t)_i|$ and i_0 is either 1 or 2 (i.e., summed over all digits or over only fingers). We are unaware of any earlier study that incorporates $\boldsymbol{F}_t$ into the objective function. Although f_1 explicitly addresses only external contact forces, this function has been proposed to be related to minimization of muscular effort (Hershkovitz et al. 1995, 1997).

3.1.2 Energylike function over $\mathbf{F_n}$—The energylike function can be expressed in terms of only $\boldsymbol{F_n}$ as:

$$f_2 = \sum_{i=i_0}^{N} (F_n)_i^2.$$

This function was selected because it has been proposed that the $\boldsymbol{F}_t$ are "passive" consequences of external loading and of the selected $\boldsymbol{F_n}$ (Pataky et al. 2004b), i.e., that the CNS is concerned only with $\boldsymbol{F_n}$ coordination. Thus the inclusion of only $\boldsymbol{F_n}$ in a cost function is appropriate. This proposal is substantiated by the fact that $\boldsymbol{F_n}$ is constrained to a greater extent by (7) than $\boldsymbol{F_t}$.

3.1.3 Entropylike function—Since it is conceivable that the CNS prefers to spread efforts as evenly as possible among redundant effectors, the entropy-motivated measure:

$$f_3 = \sum_{i=i_0}^{N} [(F_n)_i + 1] \log [(F_n)_i + 1] - \sum_{i=i_0}^{N} (F_n)_i$$

was introduced by Hershkovitz et al. (1995,1997). The equation does not represent entropy as a physical variable but was rather derived from information theory to reflect the uniformity of the contact forces.

3.1.4 Motor command function—The procedure for computing motor commands (***c***) from observed $\boldsymbol{F_n}$ has been described elsewhere (Zatsiorsky et al. 2002; cf. Danion et al. 2003b). The $N \times 1$ vector ***c*** represents the intended activation level of each finger (each $c_i \in [0, 1]$) and the manifested $\boldsymbol{F_n}$ is the result of physiological interconnections among fingers. Thus, based on the neural network model of Zatsiorsky et al. (1998), an interconnection matrix (***M***) was constructed that linearly mapped ***c*** to $\boldsymbol{F_n}$:

$$\boldsymbol{F_n} = [\boldsymbol{M}]\,\boldsymbol{c}.$$

The ***c*** can be computed based on the observed $\boldsymbol{F_n}$ by inverting the square ***M*** matrix. Thus, the objective function:

$$f_4 = \sum c_i^2$$

represents a minimization of finger "activation". This function was selected because of its physiological nature (Danion et al. 2003a) and because it has been demonstrated that f_4 more closely predicts experimental data than do other objective functions (Zatsiorsky et al. 2002).

3.1.5 Tissue deformation function—Tissue displacement minimization is significant with respect to the robotics literature, which customarily formulates grasping optimization in terms of only $\boldsymbol{F_n}$ and assumes that the $\boldsymbol{F_t}$ are passive consequences of the mechanical properties of the effectors (e.g., Hershkovitz et al. 1995). Additionally, the neural sensitivity of finger pad afferents to small strains has been well documented (e.g., Bremner et al. 1991; McNulty et al. 1999). We are unaware of any earlier study that incorporates tissue strain in an objective function.

The only data available for which the mechanical properties of the finger pads were measured for all fingers are those of Pataky et al. (2004b). However, only shear strain was measured. The authors modeled tangential tissue displacement (δ_t) as:

$$(\delta_t)_i = \frac{(F_t)_i}{m_i \cdot (F_n)_i + b_i},$$

where m and b are, respectively, the slope and intercept of linear regression of tangential stiffness on $(F_n)_i$. A cost function could be formulated as:

$$f_0 = \sum_{i=2}^{N} (\delta_t)_i^2.$$

However f_0 suffers from nonconvexity (i.e., $\nabla^2 f_0$ is not positive semidefinite). In other words, increasing $(F_n)_i$ causes a decrease in f_0. This can be avoided by including $(F_n)_i$ with a weighting coefficient (w) as a separate term in the function. The function thus becomes:

$$f_5 = \sum_{i=2}^{N} \left[w(F_n)_i^2 + (\delta_t)_i^2 \right].$$

Note that optimization results obtained using f_5 would approach those using f_2 as w gets large. For small w, f_5 approaches f_0. A value of $w = 1$ was selected such that the $(F_n)_i$ were not more important than the $(\delta_t)_i$. Ideally, tissue strain could be assessed using a finite element model (e.g., Wu et al. 2002) and incorporated in a cost function. However, such a computationally intensive analysis is inconsistent with the purposes of this paper.

3.2 Results

Typical optimization results are presented in Fig. 2. All objective functions produced qualitatively similar results: experimental $(F_n)_i$ values paralleled $(F_n)_{i*}$ with a more or less constant offset. There were exceptions to this generalization, especially for f_5 and in the vicinity of $\theta = 0°$. In particular, while experimental results transitioned smoothly from $\theta < 0°$ to $\theta > 0°$, the optimum results displayed nonsmooth transitions. The optimum thumb patterns appeared to be affected least by the cost function and also appeared to parallel experimental results most closely. This was confirmed statistically (Sect. 4.3.2).

Because of the observed offset, the typically used root-mean-square (RMS) measure was inappropriate to quantify the correspondence of experimental and optimum results. We thus introduced a new measure, the ("GSM"), which is described later (Sect. 4.3). The use of the GSM measure is justified in Sect. 4, so it is not described here. The focus will be on three experimental measures whose patterns could not be readily explained in Part I: internal force, force sharing, and SM.

3.2.1 Internal force [$(F_n)_{INT}$]—The $[(F_n)_{INT}]$ is defined as the normal force in excess of $W \sin \theta$. The experimental and optimum $(F_n)_{INT}$ results are presented in Fig. 3. These data are based on f_2 with $i_0 = 2$. As expected, optimization predicted zero $(F_n)_{INT}$ for $\theta = \pm 90°$. This was not observed in the experimental results. Consistent with the experimental results, however, was the tendency for optimized $(F_n)_{INT}$ to be slightly larger in pronated postures. Also consistent with the experimental results was the curvilinear relation of $(F_n)_{INT}$ with $\sin \theta$, although the curve was "flatter" for the optimized results in the vicinity of $\theta = 0°$. Note that a linear $(F_n)_{INT}$ vs. $\sin \theta$ relation would imply that $(F_n)_{INT}$ is a trigonometric function of θ. Thus both the larger $(F_n)_{INT}$ in pronated postures and the curvilinear relation of $(F_n)_{INT}$ and $\sin \theta$ have a purely mechanical explanation: both facts were predicted by optimization of a mechanical model.

3.2.2 Force sharing—Normal force-sharing data are presented in Fig. 4. The data represent the percentage of the total normal force produced by all four fingers. The general shapes of the experimental and optimum $(F_n)_i$-sharing vs. θ plots were quite similar. In particular, a finger's normal force-sharing percentage tended to change across the $\theta = 0$ line according to both its moment arm's magnitude and direction. That is, an $(F_n)_i$ with a "pronation moment arm" $[(r_n)_i > 0]$ tended to produce more than "even" sharing in pronation and vice versa for supination. The effect was more pronounced for larger $(r_n)_i$. Additionally, all fingers tended to return to near-constant sharing (i.e., 25%) for full supination, as predicted by optimization. Not observed in the experimental data was constant sharing for one side of the $\theta = 0°$ line ($\theta < 90°$).

3.2.3 Safety margin—The SM has been defined (e.g., Burstedt et al. 1999) as:

$$(\mathrm{SM})_i = \frac{\left((F_n)_i - \frac{|(F_t)_i|}{\mu_i}\right)}{(F_n)_i}. \tag{9}$$

The SM results derived from from $\boldsymbol{F}_*$ are reported in Fig. 5. To interpret Fig. 5, it is useful to consider the concept of weight agonists (AG) and weight antagonists (ANT). That is, T may be considered an AG for $\theta > 0$ (because $[F_n]_T$ acts to support W) and an ANT for $\theta < 0$ (because $[F_n]_T$ "adds" to W), and vice versa for the fingers. Figure 5 reveals that optimization always predicted zero SM for the ANT digits. This is unsurprising due to the nature of the inequality constraints (7). However, for all functions f, the SM for AG digits increased monotonically for $|\theta| > 0$ until its maximum value of 100% was reached at $|\theta| = 90°$. This is counterintuitive: one imagines that the "safety" level should be zero for mechanically optimum results. It seems that when an object is held with the minimum possible forces – just so the object does not slip from the hand – the SM should be zero. However, all optimization results yield nonzero SM values. This problem is addressed in the next section.

Despite the conceptual problems with the SM, Fig. 5 reveals that, for the AG digit(s), optimization SM predictions were comparably close to experimental results. The decrease in the experimental SM between $|\theta| = 75°$ and 90° can be explained by the fact that individuals produce nonzero $(F_t)_i$. En masse, the SM results indicate that slip prevention can explain the general behavior of the AG digit(s) only if a mechanically optimal solution is also considered. The SM was unable to account for the behavior of the ANT digit(s).

4 Mechanical peculiarities of nonvertical grasping

This section uses the concepts of AG and ANT (described above) to first describe the minimum normal forces required for pinch grasps and then to describe why (despite its common use in the literature) the SM is an inappropriate measure of prehension quality for nonvertical and/or multifinger grasps. In Sect. 4.2, a new measure, the GSM, is introduced. An alternative to the GSM measure, the operative friction coefficient (μ_{op}), is introduced in Sect. 4.3.3. The discussion that follows arises from a fundamental distinction: the equality constraints (8) explicitly depend on θ, while the no-slip (inequality) constraints (7) do not depend on θ.

4.1 Minimum normal forces for pinch grasp and nonvertical orientations

Consider the case of two-digit (pinch) grasp in which the T and I pinch the object shown in Fig. 1. Assume that the $(F_n)_T$ and $(F_n)_I$ are collinear such that no net moment is produced by the normal forces. In terms of the AG and ANT digits, (1)-(3) can be rewritten as follows:

$$(F_n)_{AG} - (F_n)_{ANT} - W_n = 0, \tag{10}$$

$$(F_t)_{AG} + (F_t)_{ANT} - W_t = 0, \tag{11}$$

$$-(r_t)_{AG}(F_t)_{AG} - (r_t)_{ANT}(F_t)_{ANT} = 0, \tag{12}$$

where W_n and W_t are defined in (4) and (5). Recognizing that $(r_t)_{AG} = (r_t)_{ANT}$, rearranging (12) and substituting it into (11) yields:

$$(F_t)_{AG} = (F_t)_{ANT} = \frac{1}{2} W_t. \tag{13}$$

Since the $(F_t)_{ANT}$ must be equal to half of the projection of W on the t axis, the minimum ANT normal force is given by:

$$\left[(F_n)_{\mathrm{ANT}}\right]_{\min}=\mu^{-1}(F_t)_{\mathrm{ANT}}=(2\mu)^{-1}W_t \tag{14}$$

because the ANT finger is subjected to the no-slip constraint (4). Note that in this situation of pinch grasp with no moments being produced by normal forces, the ANT finger must produce normal force, thereby adding to W. The same would be true for multifinger grasping if the VF could not change its point of force application by redistributing the normal forces among the fingers. The result of (14), when substituted into (10) yields:

$$\left[(F_n)_{\mathrm{AG}}\right]_{\min}=\left[(F_n)_{\mathrm{ANT}}\right]_{\min}+W_n=(2\mu)^{-1}W_t+W_n. \tag{15}$$

Note that the AG force is indeed a minimum in (15) because W_n is always greater than zero. Since only $(2\mu)^{-1}$ W_t units of $(F_n)_{\mathrm{AG}}$ are sufficient to prevent slip [see (14)], the AG finger would never slip (if the frictional conditions are identical at the two digits). This is because AG slip prevention is an inevitable consequence of equilibrium Eq. (1). A simple experiment could confirm this physical fact: during pinch grasp of an object held at $\theta \neq 0$, one cannot voluntarily slip the AG finger without first accelerating the object toward the AG finger [by virtue of (15)]. The SM thus seems ambiguous for the AG digit, despite the similarities between experimental and predicted SM values (Fig. 5) discussed in Sect. 3.2.3. The apparently dual roles of $(F_n)_{\mathrm{AG}}$ for W support and for slip prevention are therefore actually physically inseparable in static pinch grasp. Defining a critical angle θ at which the role of the $(F_n)_{\mathrm{AG}}$ changes from one of slip prevention to one of W support is thus superfluous.

A graphical interpretation of (14) and (15) presented in Fig. 6 reveals the inherent nonlinearities of these equations. The minimum normal forces of individual fingers are nontrigonometric functions of θ, and μ obviously affects the shape of these functions. There is also a non-smooth transition in each digit's behavior across the $\theta = 0$ line.

Figure 6 and (14) and (15) illustrate that the minimum $(F_n)_{\mathrm{AG}}$ finger force clearly depends on many factors including W, θ, μ, and the selected $(F_n)_{\mathrm{ANT}}$ – which must be at least $[(F_n)_{\mathrm{ANT}}]_{\min}$. Even this simple and idealized model has inherently highly complex mechanics.

4.2 Problems with the safety margin (SM) measure for nonvertical orientations

The literal interpretation of (9) – as stated in Sect. 2.4.2.2 of Part I of this study – is as follows: the SM is the proportion of a digit's exerted normal force that is not functioning for slip prevention. This interpretation is valid for all θ. However, (9) has implicit meaning beyond this literal interpretation. An alternative interpretation arises because of the peculiarities of the task mechanics (7) and (8) and because of the literature's original intended use of the SM for $\theta = 0$ and for pinch grasp:

Alternative interpretation of the SM (as stated in Sect. 1): The SM is the proportion of a digit's F_n that exceeds the task-dependent minimum F_n. This interpretation accounts for the inseparability of the finger forces' dual roles of weight support and slip prevention when $\theta \neq 0$. We believe that this interpretation represents the essence of the original intended meaning of the SM. Note that the alternative interpretation is consistent with the literal interpretation for $\theta = 0$. A mechanical analysis supports these ideas.

Assume that the CNS solves the two-digit pinch problem of Sect. 4.1 in exactly the way described in (14) and (15). If an experimenter were to quantify the SM as it appears in (9), the results would be as in Fig. 7 (for $\mu = 1.4$). As in Fig. 5, when a digit acts as an ANT, the predicted

SM is zero, as one would expect. However, when the finger is an AG, the SM is nonzero, and in fact reaches its maximum possible value of unity for $\theta = 90°$.

This is paradoxical: the subject chooses the mechanically minimum normal force acting against the load, $(F_n)_{AG}$, and yet his/her SM is nonzero. This paradox, we argue, is precisely the reason why (9) does not capture the essence of the SM. We thus propose a new measure that we believe does capture the intended meaning of the SM and that can be generalized to both nonvertical and multifinger grasping: the GSM.

4.3 Generalized safety margin

Because of the conceptual problems of the SM described above, we would like to introduce the generalized safety margin (GSM) as a means to quantify prehension quality. The GSM is calculated as:

$$(\mathrm{GSM})_{i,q} = \frac{\left(F_q\right)_i - \left(F_q\right)_i^*}{\left(F_q\right)_i^*}, \tag{16}$$

where $(F_q)_i$ is the observed force of the ith finger along an arbitrary axis (q), and $(F_q)_{i*}$ is the optimum force determined by minimization of some objective function. The subscript i, q on GSM indicates that the GSM can be calculated for each digit and each axis separately. We use the term "scaling" in GSM because experimental data indicated that the GSM was never zero; rather experimental data seemed to have a constant offset from optimal data. The similarities between (16) and (9) are apparent; it can be shown that (16) reduces to (9) for $\theta = 0$ and for pinch grasp. Importantly, if a subject selects the mechanically minimum forces prescribed by (14) and (15), the GSM would be zero. The GSM thus maintains the essence of the SM meaning while genera lizing the SM calculation to both $\theta \neq 0$ and multifingered grasping.

4.3.1 GSM results—To quantify the quality of fit between the predicted optimal and experimentally observed finger forces, the GSM measure was introduced (Sect. 3.1). A single GSM value was calculated for each i, q combination and for each θ. The mean normalized by $W(F_q)_i$ was computed for each θ.

As a demonstration of the GSM concept applied to experimental data, example optimization results appear in Fig. 8 for f_2 and for $i_0 = 2$ (refer to Fig. 2 for the $\boldsymbol{F}_n$ and $\boldsymbol{F}_{n*}$ data). No statistical tests were performed on the results presented in Fig. 8 – these data are simply intended to illustrate the concept of the GSM. It is apparent that the GSM is larger for $\theta = 0$ vs. $\theta \neq 0$ for all digits except I. It is also apparent that T has the largest and most variable GSM for both axes; note that the $(\mathrm{GSM}_n)_T$ is equal to the $(\mathrm{GSM}_n)_{VF}$.

4.3.2 "Best" objective function?—The quality of fit between optimum and experimental data was determined as follows: the average $(\mathrm{GSM}_n)_i$ was added to each $(F_n^*)_i$ to produce $\boldsymbol{F}_{n*}$ + GSM curves. The quality of fit for a given digit was then determined as the RMS between the experimental $(F_n)_i$ curve and the $(F_n)_i^*$+GSM curve. This is analogous to quantifying the similarities in curve shapes across θ. Since GSM_t values (not yet presented) were much lower than GSM_n values, the RMS was computed between the unmodified $\boldsymbol{F}_t$ and $\boldsymbol{F}_{t*}$ curves.

The RMS data are presented in Table 1. The tissue displacement cost function f_5 was not included in the analysis because of its dissimilar results (Fig. 2) and because a complete tissue strain measure could not be described parametrically (Sect. 3.1.5). All other functions produced very similar RMS values for a given digit and a given direction (i.e., n or t). Interestingly, the RMS values for $(F_n)_T$ were consistently the lowest. This might be due to the fact that there are

no redundant effectors acting in parallel with $(F_n)_T$. At a significance level $\alpha = 0.05$, analysis of variance (ANOVA) confirmed that different functions did not affect the RMS values: p values were greater than 0.13 for all $(F_n)_i$ except for the I finger ($p = 0.031$), and p values were greater than 0.556 for all (F_{ti}. Additionally, the RMS values were not affected by i_0 for all $(F_q)_i (p > 0.130)$. Thus all cost functions yielded statistically similar results.

4.3.3 Alternative interpretation of GSM: operative friction coefficient—Rather than performing optimization and then scaling the results, as suggested above, the CNS could alternatively employ an operative friction coefficient (μ_{op}) that would describe the GSM. By assumption, the μ_{op} – which is different from the actual μ – is a coefficient that the CNS uses when it determines finger forces. That is, if the CNS assumes that there is a μ lower than the actual μ, then the $\boldsymbol{F_{n^*}}$ solutions would be driven upward toward the experimental data. This μ_{op} thus reflects a SM of sorts. The intuitive appeal of the μ_{op} over either the SM or GSM measure is that the latter measures imply that the CNS stores some scaling number; the μ_{op} contrastingly reflects the fact that the CNS does not have explicit knowledge of the actual μ.

The μ_{op} that might be used by the CNS can be computed for each digit based on the relation between RMS and the μ that is submitted to an optimization routine. That is, the RMS of the difference between $\boldsymbol{F_n}$ and $\boldsymbol{F_{n^*}}$ is computed as a function of μ (note that this RMS differs from the one used in Sect. 4.3.2). The μ_{op} is then the μ for which the RMS is a minimum.

Figure 9a illustrates the relation between RMS and μ_{op}. The figure indicates that the RMS reaches local minima for μ_{op} in the range 0.33 to 0.7. A μ_{op} value of 0.4 produces quite low RMS values for all digits. Therefore, if CNS assumes that the μ is 30% of its actual value, the experimental and optimal data have the closest agreement. The optimization results corresponding to $\mu_{op} = 0.4$ are shown in Fig. 9b. While these $\boldsymbol{F_{n^*}}$ results are certainly *closer* to the experimental data than the $\boldsymbol{F_{n^*}}$ results shown in Fig. 2, there are still discrepancies. Note especially that for $|\theta| = 90°$, optimization unsurprisingly still predicts zero ANT force.

5 Discussion

The present study yielded three main findings:

1. The GSM, herein introduced, is a more broadly applicable measure than the typically used SM for quantifying prehension quality.
2. Various cost functions yield optimization results that are in good qualitative agreement with experimental force data obtained during nonvertical grasping.
3. Assuming that the CNS views an object as being more slippery than it is, in conjunction with optimization, can partially account for the offset between experimental and optimal data.

The first main finding, that the GSM is a better measure than the SM, is justified because the former can be generalized to nonvertical and multifinger grasps while preserving the meaning of the latter. Indeed the GSM reduces to the SM for vertical orientations and two-digit grasps. The remainder of the discussion addresses the second and third main findings.

Many of the human behaviors observed in Part I of this study (Pataky et al. 2004a) were explained by a purely mechanical analysis of nonvertical grasping. These behaviors included, among others, greater internal force for pronated postures, nonzero agonist SM, and the general patterns of force sharing among the redundant fingers. The difference in optimum forces between fingers emerged simply because of their different moment arms.

The finding that several cost functions worked equally well is consistent with a previous study that only found cost function differences for large external torques (Zatsiorsky et al. 2002). The finding that tissue displacement minimization did not produce good agreement with experimental data is significant because the grasp-planning algorithms proposed in the robotics literature are concerned primarily with normal forces; tangential forces are passive consequences of the structural properties of the effectors (e.g., Hershkovitz et al. 1995). Although tissue displacement minimization cannot explain the observed finger forces, perhaps more sophisticated models of the passive properties of the fingers could.

Of the experimental behaviors not explained by optimization, the most apparent was the more or less constant offset between experimental and optimum data (i.e., a constant GSM). The selective stabilization of the GSM, if real, suggests that at least two CNS processes may be responsible for the observed prehension synergies: (1) determining an optimal solution and (2) scaling the solution. The former does not imply that the CNS performs the mathematical operations described by optimization; it rather implies that finger forces map to some internal neural representation, and it is these variables that are fine-tuned by the system such that small changes in forces result in the increase of a perceivable signal. The process of force-to-neural mapping has physiological merit: forces are sensitively detected by mechanoreceptors in the finger pads and can be integrated by the CNS (McNulty et al. 1999). Additionally, it has been found that force is represented in the motor cortex (Asanuma 1973; Evarts 1973; Schieber et al. 2001).

The physiological basis for the GSM scaling process is more elusive. It is possible that the GSM arises from mechanisms similar to those that have been hypothesized to be responsible for the SM (Westling and Johansson 1984): psychological/mechanical factors including the desire for grasp stability, specifically the tendency to reduce the effects of potential external disturbances. If such a mechanism operates, it would be interesting to know whether grasping a vibrating object is associated with larger GSM. Explaining the cause of the GSM is certainly not trivial: even a more mathematically rigorous formulation of prehension optimization could not explain the scaling observed in human performance without incorporating a GSM-like measure (Hershkovitz et al. 1997).

Perhaps a more intuitively appealing account of the GSM is the following: if the CNS assumes that an object has some arbitrarily high slipperiness, then measures like the SM and GSM would naturally emerge, without explicit knowledge of either friction or the optimum solution. This idea is described herein by the operative friction coefficient. This new variable cannot, obviously, explain all the data: optimization still predicts zero normal forces for horizontal orientations. However, the present model is phenomenological and contains no anatomy or physiology (with the exception of the motor commands of Zatsiorsky et al. 1998); the fingers differ only in the moment arms with respect to the object's axis of rotation. While a more sophisticated biomechanical model might explain the data more completely, the successes of the present model collectively represent a useful starting point.

The implications of the optimization-derived variables beget a plethora of empirical questions. In short, any experimental manipulation (e.g., changed friction, nonzero external moment, etc.) is expected to change the optimum forces. Whether the experimental forces follow the task-dependent optimum forces is unknown.

All optimization models suffer from the interdependence of the design variables. That is, slightly changing one finger force affects all other finger forces. Thus if a subject performs exactly optimally and then slightly changes one finger force, the quality of fit between experimental and optimum data balloons. It is precisely because of this interdependence problem that we were surprised to observe that all fingers closely paralleled the optimum results

when no interfinger differences were incorporated into the model. Each finger has different geometry and hence different gross muscle architecture, and each finger also has different mechanical performance characteristics (e.g., Li et al. 1998). The parallel between experimental and optimal finger forces thus reflects a relation that transcends anatomy and follows mechanical principles. Solutions rendered by optimization of mechanically redundant models of prehension therefore appear to be promising resources for aiding interpretation of experimental human performance.

Acknowledgments

Supported in part by NIH grants AR-48563, AG-018751, and NS-35032.

References

Arbib MA, Iberall T, Lyons D. Coordinated control programs for movements of the hand. Exp Brain Res Suppl 1985;10:111–129.

Asanuma H. Cerebral cortical control of movements. Physiologist 1973;16:143–166. [PubMed: 4197405]

Belegundu, AD.; Chandrupatla, TR. Optimization concepts and applications in engineering. Prentice-Hall; Englewood Cliffs, NJ: 1999.

Bremner FD, Baker JR, Stephens JA. Correlation between the discharges of motor units recorded from the same and from different finger muscles in man. J Physiol 1991;432:355–380. [PubMed: 1886059]

Burstedt MK, Flanagan JR, Johansson RS. Control of grasp stability in humans under different frictional conditions during multidigit manipulation. J Neurophysiol 1999;82(5):2393–2405. [PubMed: 10561413]

Danion F, Latash ML, Li S. Finger interactions studied with transcranial magnetic stimulation during multi-finger force production tasks. Clin Neurophysiol 2003a;114:1445–1455. [PubMed: 12888027]

Danion F, Schoner G, Latash ML, Li S, Scholz JP, Zatsiorsky VM. A mode hypothesis for finger interaction during multi-finger force-production tasks. Biol Cybern 2003b;88(2):91–98. [PubMed: 12567224]

Evarts EV. Motor cortex reflexes associated with learned movement. Science 1973;179:501–503. [PubMed: 4196171]

Hershkovitz M, Tasch U, Teboulle M. Toward a formulation of the human grasping quality sense. J Robot Syst 1995;12(4):249–256.

Hershkovitz M, Tasch U, Teboulle M, Tzelgov J. Experimental validation of an optimization formulation of the human grasping quality sense. J Robot Syst 1997;14(11):753–766.

Iberall, T. The representation of objects for grasping; Proceedings of the 8th Cognitive Society conference; 1986; p. 547-561.

Latash ML, Gelfand IM, Li ZM, Zatsiorsky VM. Changes in the force-sharing pattern induced by modifications of visual feedback during force production by a set of fingers. Exp Brain Res 1998;123(3):255–262. [PubMed: 9860263]

Li ZM. Inter-digit co-ordination and object-digit interaction when holding an object with five digits. Ergonomics 2002;45(6):425–440. [PubMed: 12061967]

Li ZM, Latash ML, Newell KM, Zatsiorsky VM. Motor redundancy during maximal voluntary contraction in four-finger tasks. Exp Brain Res 1998;122(1):71–78. [PubMed: 9772113]

Li ZM, Zatsiorsky VM, Latash ML. Contribution of the extrinsic and intrinsic hand muscles to the moments in finger joints. Clin Biomech 2000;15(3):203–211.

McNulty PA, Turker KS, Macefield VG. Evidence for strong synaptic coupling between single tactile afferents and motoneurones supplying the human hand. J Physiol 1999;518(3):883–893. [PubMed: 10420022]

Pataky TC, Latash ML, Zatsiorsky VM. Prehension synergies during non-vertical grasping. I. Experimental observations. Biol Cybern 2004a;91:148–158. [PubMed: 15378373]

Pataky TC, Latash ML, Zatsiorsky VM. Tangential load sharing among fingers during prehension. Ergonomics 2004b;47(8):876–889. [PubMed: 15204280]

Pataky TC, Latash ML, Zatsiorsky VM. Viscoelastic response of the finger pad to incremental tangential displacements. J Biomech. 2004c in press.

Schieber MH. Constraints on somatotopic organization in the primary motor cortex. J Neurophysiol 2001;86:2125–2143. [PubMed: 11698506]

Shim JK, Latash ML, Zatsiorsky VM. Prehension synergies: trial-to-trial variability and hierarchical organization of stable performance. Exp Brain Res 2003;152(2):173–184. [PubMed: 12898101]

Westling G, Johansson RS. Factors influencing the force control during precision grip. Exp Brain Res 1984;53(2):277–284. [PubMed: 6705863]

Wu JZ, Dong RG, Rakheja S, Schopper AW. Simulation of mechanical responses of fingertip to dynamic loading. Med Eng Phys 2002;24(4):253–264. [PubMed: 11996844]

Zatsiorsky VM, Gregory RW, Latash ML. Force and torque production in static multifinger prehension: biomechanics and control. II. Control. Biol Cybern 2002;87(1):40–49. [PubMed: 12111267]

Zatsiorsky VM, Li ZM, Latash ML. Coordinated force production in multi-finger tasks: finger interaction and neural network modeling. Biol Cybern 1998;79(2):139–150. [PubMed: 9791934]

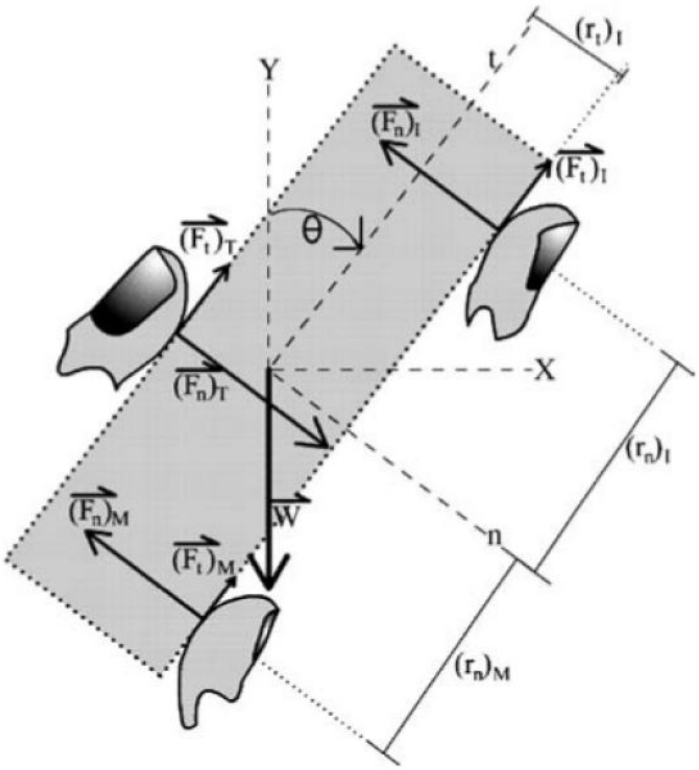

Fig. 1.

Coordinate systems and notation used. The local normal (*n*) and tangential (*t*) axes are coincident with global horizontal (*X*) and vertical (*Y*), respectively, for orientation $\theta = 0$. The normal and tangential forces (F_n and F_t, respectively) are shown for the thumb and the index and middle fingers (T, I, and M, respectively). Moment arms (*r*) about the origin are shown for F_n and F_t separately, but not for all digit forces

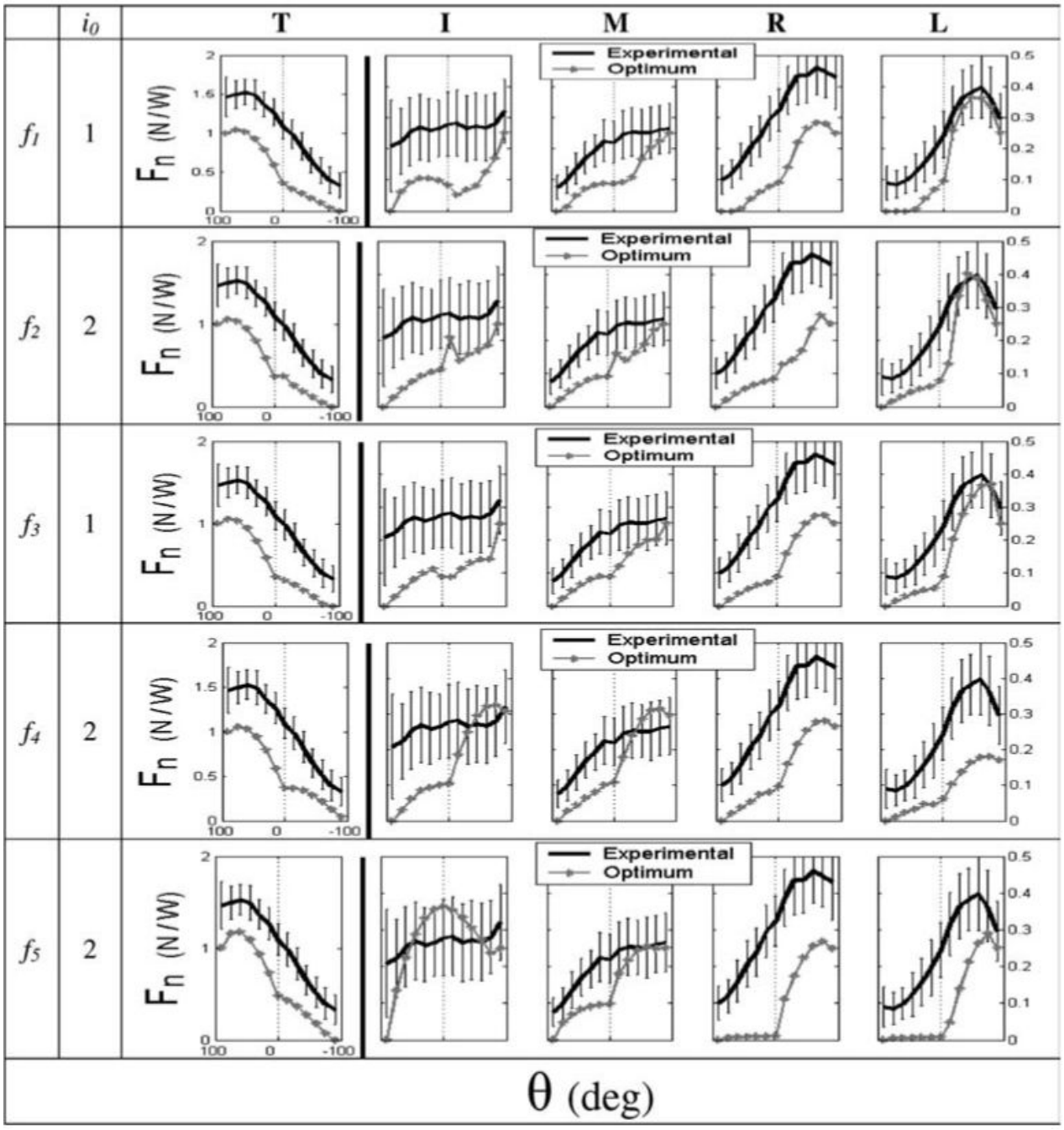

Fig. 2.

Exemplary $\boldsymbol{F_{n^*}}$ optimization results (*gray*) for the five objective functions (*f* – see text for a description of the functions). Each function incorporates different digits: $i_0 = 1$ indicates that the T and all fingers were used, and $i_0 = 2$ indicates that only the fingers were used. Different digits are presented in different columns. Experimental data are shown in *black* as a reference; *error bars* represent standard deviations. Note the different force scales for the T (*left*) and the fingers (*right*). All plots have $\theta > 0$ to the left of the ordinate to be consistent with figures from Part I of this study

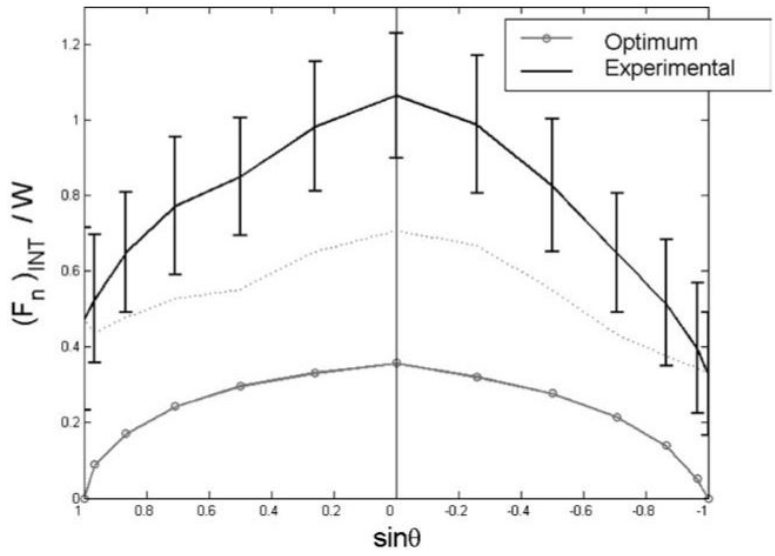

Fig. 3.

Internal normal force computed from experimental $\boldsymbol{F}$ data (*black*) and from $\boldsymbol{F}_*$ (*gray*) for objective function f_2 with $i_0 = 2$ (i.e., fingers only without thumb). The *dotted line* represents the difference between the average experimental $(F_n)_{\mathrm{INT}}$ and that calculated from $\boldsymbol{F}_*$. Data are presented, as in Part I of this study, as a function of sin θ

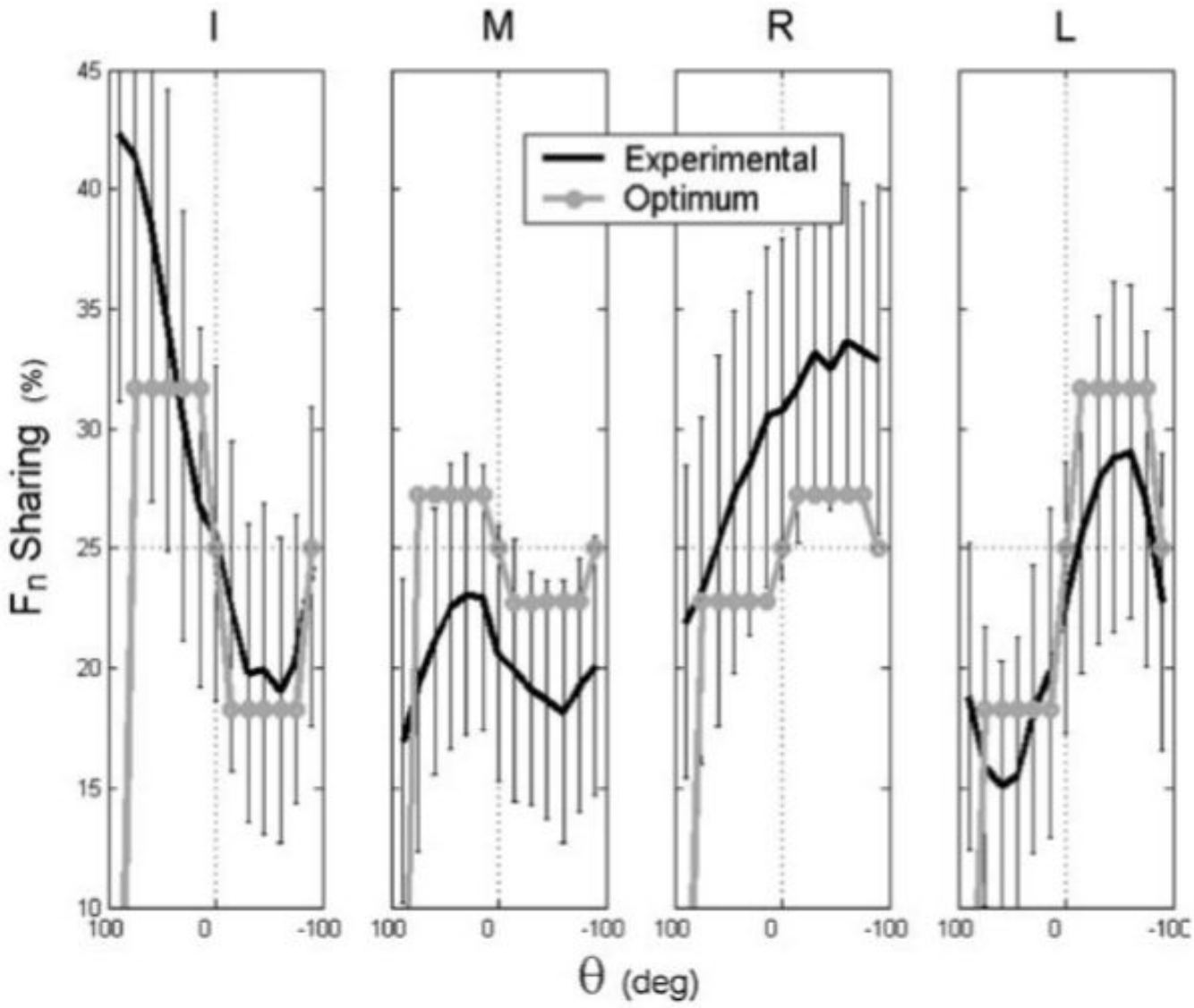

Fig. 4.

Force sharing computed from experimental ***F*** data (*black*) and from $\boldsymbol{F}_*$ (*gray*) for objective function f_2 with $i_0 = 2$. The *horizontal dotted lines* indicate even sharing among the digits (i.e. 25%)

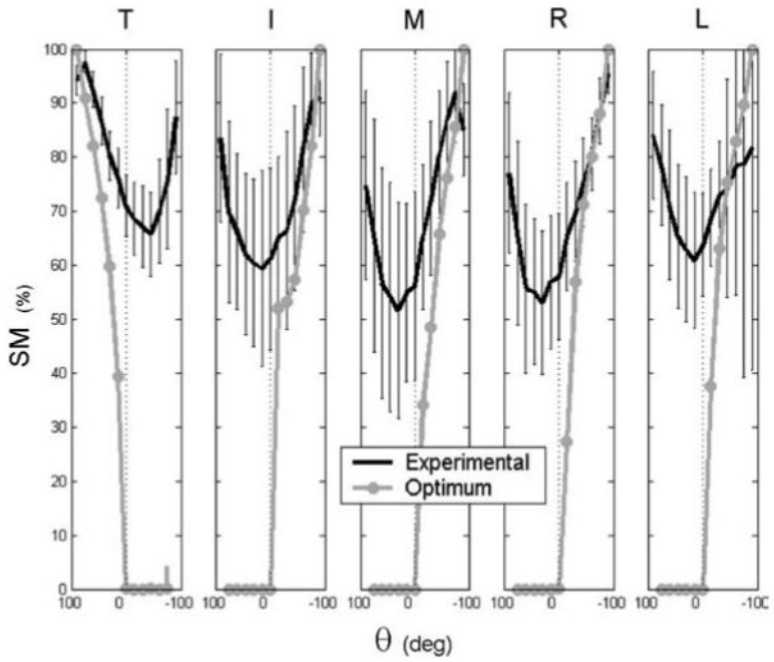

Fig. 5.
Safety margin computed from experimental $\boldsymbol{F}$ data (*black*) and from $\boldsymbol{F}_*$ (*gray*) for objective function f_2 with $i_0 = 2$

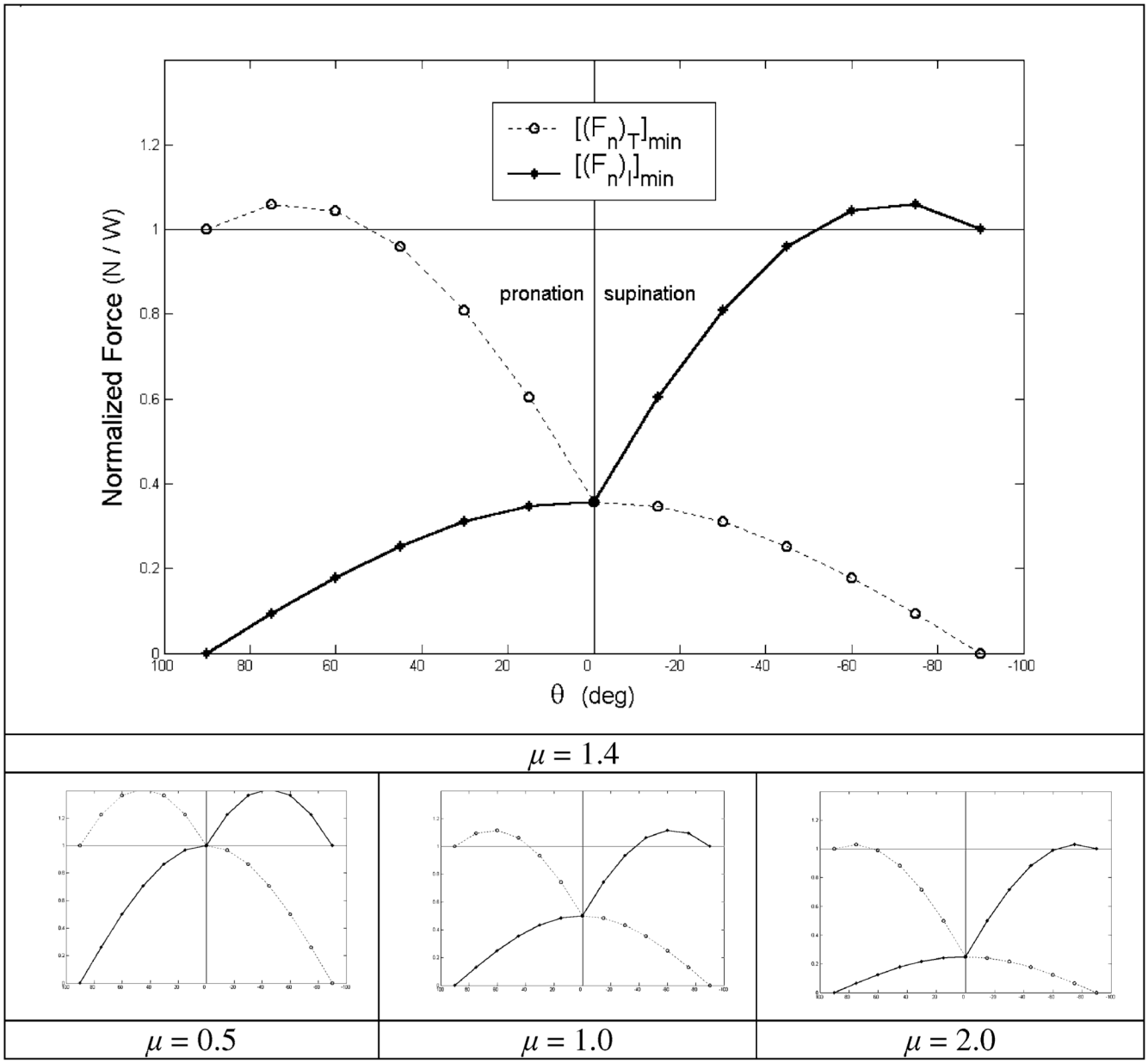

Fig. 6.

Minimum normal forces of T and I fingers for a pinch grasp in which normal forces exert no net moment. The *top panel* shows the minimum finger forces for the coefficient of friction (μ) used in the experiment of Part I of this study (current issue). The *bottom panels* show the effect of μ on the minimum forces. Note that $\theta > 0$ appears to the left of the ordinate

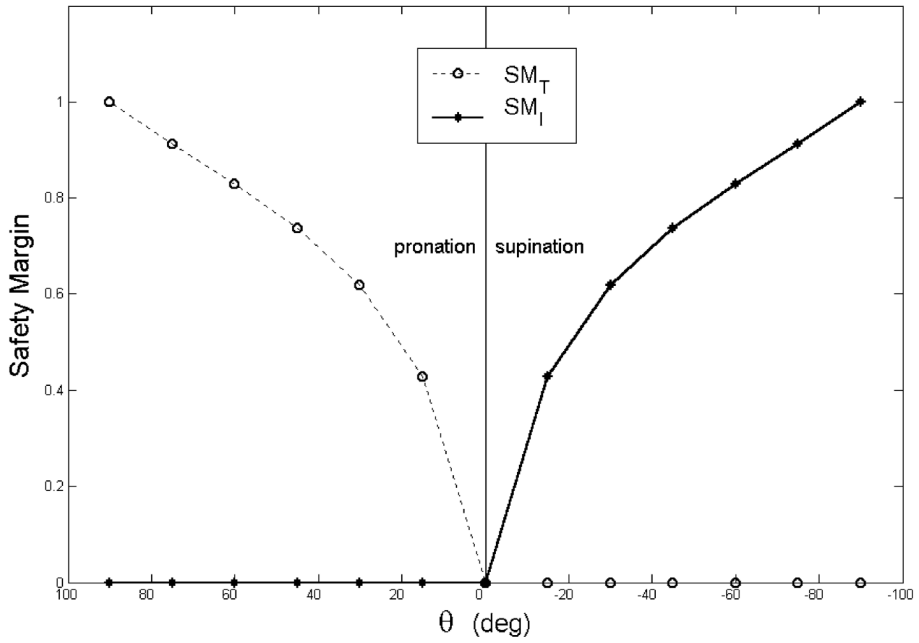

Fig. 7.
Safety margin computed from the minimum force of Fig. 2 for $\mu = 1.4$

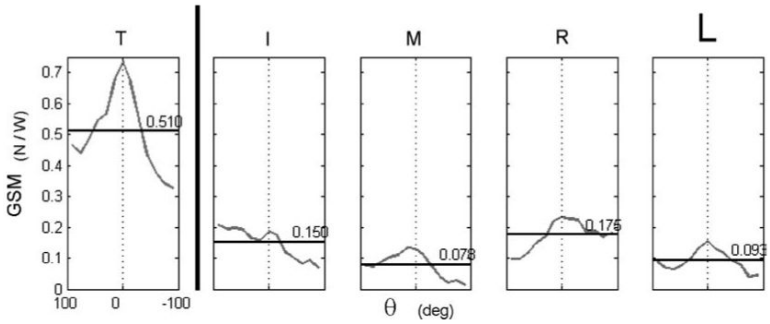

Fig. 8.

Exemplary GSM results. The objective function used here was f_2 with $i_0 = 2$. The average GSM is indicated by a horizontal line and its value is printed at the right side of each *lower panel*. The standard deviations of GSM across θ were: 0.137, 0.052, 0.043, 0.048, and 0.036 for the T, I, M, R, and L digits, respectively

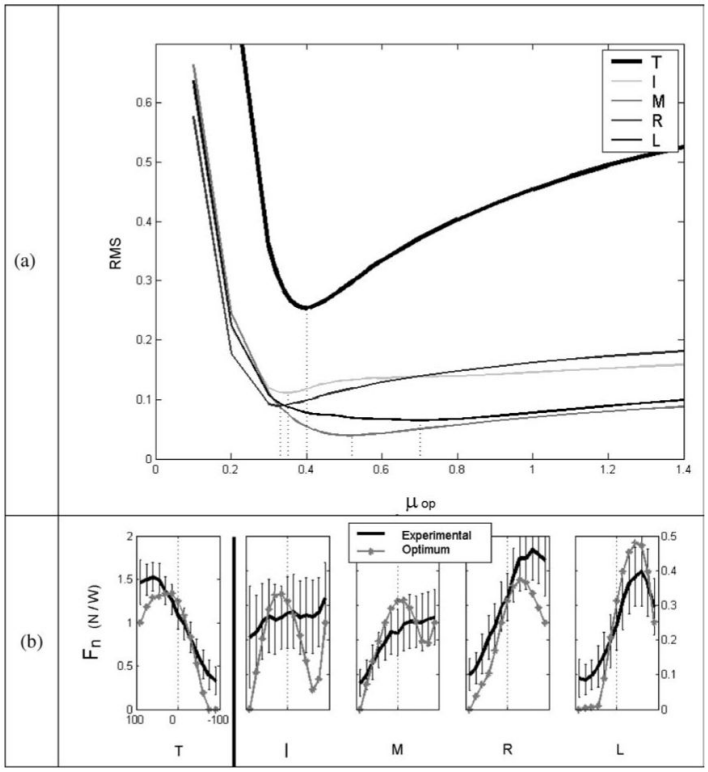

Fig. 9a, b.

a RMS between experimental $\boldsymbol{F}_n$ and optimized $\boldsymbol{F}_{n*}$ as a function of the operative friction coefficient (μ_{op} – see text). The cost function used was f_2 with $i_0 = 2$. The *dotted vertical lines* show the μ_{op} values for which different digits have a minimum RMS. These minimum μ_{op} values range from 0.33 for the R finger to 0.7 for the L finger. **b** Optimization results for $\mu_{op} = 0.4$ and experimental data

Table 1

Root-mean-square (dimensionless units: *N/W*) between experimental $\boldsymbol{F}$ values and optimum $\boldsymbol{F}_*$ results

Cost function:	f_1	f_1	f_2	f_2	f_3	f_3	f_4
i_0	**1**	**2**	**1**	**2**	**1**	**2**	**2**
$(F_n)_T$	0.124	0.124	0.133	0.125	0.121	0.128	0.143
$(F_n)_I$	0.536	0.539	0.537	0.538	0.536	0.537	0.547
$(F_n)_M$	0.428	0.433	0.432	0.431	0.429	0.427	0.442
$(F_n)_R$	0.665	0.661	0.668	0.662	0.662	0.667	0.663
$(F_n)_L$	0.547	0.529	0.547	0.534	0.542	0.559	0.513
$(F_t)_T$	0.086	0.078	0.102	0.074	0.079	0.106	0.097
$(F_t)_I$	0.024	0.021	0.074	0.027	0.028	0.061	0.028
$(F_t)_M$	0.037	0.027	0.048	0.031	0.035	0.043	0.019
$(F_t)_R$	0.049	0.053	0.087	0.047	0.046	0.078	0.057
$(F_t)_L$	0.027	0.013	0.047	0.014	0.018	0.053	0.021

The RMS for $\boldsymbol{F_n}$ was determined based on the $\boldsymbol{F_n}_*$ plus the average *OSF* (see text). The cost functions f_j are defined in Sect. 3.1. The index i_0 indicates whether the cost functions incorporated all digits (i_0 = 1) or only the fingers (i_0 = 2). Function f_5 was not included for reasons described in Sect. 4.3.2.